Superconductivity and charge density wave order in the two-dimensional Holstein model

Owen Bradley, George G. Batrouni, and Richard T. Scalettar

Phys. Rev. B **103**, 235104 — Published 1 June 2021

DOI: 10.1103/PhysRevB.103.235104

Superconductivity and charge density wave order in the 2D Holstein model

Owen Bradley,[1] George G. Batrouni,[2,3,4,5] and Richard T. Scalettar[1]

[1] *Department of Physics, University of California Davis, CA 95616, USA*
[2] *Université Côte d'Azur, CNRS, Institut de Physique de Nice, Nice, France*
[3] *Centre for Quantum Technologies, National University of Singapore, 2 Science Drive 3, 117542 Singapore*
[4] *Department of Physics, National University of Singapore, 2 Science Drive 3, 117542 Singapore*
[5] *Beijing Computational Science Research Center, Beijing 100193, China*

(Dated: April 6, 2021)

The Holstein Hamiltonian describes fermions hopping on a lattice and interacting locally with dispersionless phonon degrees of freedom. In the low density limit, dressed quasiparticles, polarons and bipolarons, propagate with an effective mass. At higher densities, pairs can condense into a low temperature superconducting phase and, at or near commensurate filling on a bipartite lattice, to charge density wave (CDW) order. CDW formation breaks a discrete symmetry and hence occurs via a second order (Ising) transition, and therefore at a finite $T_{\rm cdw}$ in two dimensions. Quantum Monte Carlo calculations have determined $T_{\rm cdw}$ for a variety of geometries, including square, honeycomb, and Lieb lattices. The superconducting transition, on the other hand, in $d = 2$ is in the Kosterlitz-Thouless (KT) universality class, and is much less well characterized. In this paper we determine $T_{\rm sc}$ for the square lattice, for several values of the density ρ and phonon frequency ω_0. We find that quasi-long range order sets in at $T_{\rm sc} \lesssim t/20$, where t is the near neighbor hopping amplitude, consistent with previous rough estimates from simulations which only extrapolated to the temperatures we reach from considerably higher T. We also show evidence for a discontinuous evolution of the density as the CDW transition is approached at half-filling.

I. INTRODUCTION

The interactions of electrons with lattice degrees of freedom (phonons) underlie many of the fundamental properties of solid state materials. The many-body nature of the problem, however, poses significant challenges to analytic investigation. Hence, over the last several decades, increasingly sophisticated computational methods have been exploited to gain quantitative insight. Early quantum Monte Carlo (QMC) work on electron-phonon models focused on the dilute limit. As an electron moves through a material, the polarization of the underlying medium causes a cloud of phonons to follow. Simulations studied the resulting "single electron polaron", identifying its size and effective mass as functions of the electron-phonon coupling and phonon frequency [1–9]. If the interaction is sufficiently large, it was shown that it is possible for two polarons to pair. The size, dispersion, and stability of the resulting bipolarons was evaluated [10–12], as well as bipolaron physics across a range of fillings [13].

As the density of these dressed quasiparticles increases, they can condense into phases with long range order (LRO). One possibility is off-diagonal quasi-long range order, i.e. superconductivity (SC). At, and close to, special commensurate densities, on a bipartite lattice, diagonal LRO, i.e. charge density wave (CDW) states, are another possibility. The competition between these two low temperature phases is a fundamental feature of both materials [14–16] and of simplified models of the electron-phonon interaction.

One such model is the Holstein Hamiltonian [17], which describes electrons hopping on a lattice and interacting locally with dispersionless phonon degrees of freedom. At commensurate filling on bipartite lattices, it exhibits a transition to CDW order at a finite $T_{\rm cdw}$ in two dimensions. Early QMC studies of the Holstein model examined the competition between CDW and SC on square lattices of up to 8×8 sites, observing the enhancement of SC correlations and a simultaneous reduction in the CDW structure factor as the system is doped away from half-filling [18–20]. Early estimates of $T_{\rm cdw}$ were obtained using a finite-size scaling approach, although computational constraints on lattice size limited their accuracy.

The SC transition believed to occur away from half-filling (in two dimensions) belongs to the Kosterlitz-Thouless (KT) universality class. Although similar attempts were made to quantify its appearance, it remains much less well characterized. Vekić et. al [20] provided estimates for $T_{\rm sc}$ based on a finite-size scaling of QMC data for the same lattices of up to 8×8 sites, as were analyzed for the CDW transition, but only reached inverse temperatures $\beta \leq 12/t$. The computational limitations on both temperature and lattice size which restricted simulations to these ranges prevented an accurate finite-size scaling to be performed. For phonon frequencies $\omega_0/t = 1$, it was estimated that the SC transition occurs within an approximate range $\beta_{\rm sc} = 30$–40, more than a factor of two colder than the lowest temperatures simulated. Finite-size scaling estimates of the critical temperature at higher phonon frequencies, which would tend to have higher, and hence more accessible, $T_{\rm sc}$ were also limited in accuracy.

More recent studies of the Holstein model have refined estimates of $T_{\rm cdw}$ at half-filling on the square lattice [21–

23], and studied the interplay between SC and CDW order as electron-phonon coupling is varied [24]. The influence of phonon dispersion on both SC and CDW ordering has also been studied [23], with strong evidence found for the onset of SC at half-filling when phonon dispersion is present. A finite-size scaling analysis obtained $T_{\rm sc} \approx t/26$ at a phonon frequency $\omega_0/t = 4$, simulating lattices of up to 12×12 sites. Recently, the CDW transition in the Holstein model has also been investigated for both the honeycomb and π-flux geometries [25–27], as well as for the square lattice with anisotropic hopping amplitudes [28]. These studies focused on the half-filled case only and hence did not advance our understanding of $T_{\rm sc}$. Recent work on the triangular lattice Holstein model [29] has shown that frustrating the charge order via a non-bipartite lattice can enhance SC, and an estimate of $T_{\rm sc} \approx t/10$ was obtained at a phonon frequency $\hbar\omega/E_F = 0.3$ (where E_F is the Fermi energy). This estimate was obtained at half-filling through a finite-size scaling analysis, using lattices up to 12×12 sites. However, in the work of [29], no analogous evidence of the SC transition was observed for the square lattice for the parameters studied.

In the present paper, we resolve this situation by determining $T_{\rm sc}$ for the square lattice for several values of the phonon frequency ω_0 and electron density ρ away from half-filling. We perform QMC simulations of lattices up to 12×12 sites, at inverse temperatures up to $\beta = 28/t$. Through a finite-size scaling analysis we find that SC sets in close to the lowest temperatures simulated. That is, our study does not rely on an extrapolation from temperatures much higher than $T_{\rm sc}$. We also investigate the variation of the CDW structure factor with wave vector as the system is doped away from half-filling, finding evidence for a possible incommensurate CDW phase at low temperature.

We note that, in addition to the computational literature cited above, considerable effort has gone into the analytic solution of the Holstein Hamiltonian. The Migdal-Eliashberg (ME) equations [30, 31] form the basis for much of the analytic work on strongly coupled electron-phonon models, but disagree with exact QMC simulations [18–20, 32, 33], especially as the temperature is lowered at densities in the vicinity of half-filling where competing CDW formation occurs. This comparison can be improved somewhat with 'renormalized ME' theory in which the phonon propagator is dressed by electron-hole bubbles [34]. Recently, there has been renewed interest in examining the limits of ME theory and when it breaks down [35–39]. Indeed, it has been shown that ME can work well for $\omega_0 << E_F$ provided the electron phonon coupling is not too large, enabling estimates of T_{SC} to be made by extrapolating DQMC results down to lower temperatures using ME calculations [35]. However, we note that several of the parameter sets we study in this work are outside the limits of ME theory.

II. MODEL AND METHODS

The Holstein model is a tight-binding Hamiltonian which describes the interaction between electrons and local phonon modes in a lattice [17],

$$\hat{H} = -t \sum_{\langle \mathbf{i},\mathbf{j}\rangle,\sigma} \left(\hat{c}^\dagger_{\mathbf{i}\sigma} \hat{c}_{\mathbf{j}\sigma} + h.c. \right) - \mu \sum_{\mathbf{i}\sigma} \hat{n}_{\mathbf{i}\sigma} + \frac{1}{2} \sum_{\mathbf{i}} \hat{P}^2_{\mathbf{i}} + \frac{\omega_0^2}{2} \sum_{\mathbf{i}} \hat{X}^2_{\mathbf{i}} + \lambda \sum_{\mathbf{i}\sigma} \hat{n}_{\mathbf{i}\sigma} \hat{X}_{\mathbf{i}} \, . \quad (1)$$

Here $\hat{c}^\dagger_{\mathbf{i}\sigma}(\hat{c}_{\mathbf{i}\sigma})$ are creation (destruction) operators for an electron at site $\mathbf{i}$ with spin σ, μ is the chemical potential, and $\hat{n}_{\mathbf{i}\sigma} = \hat{c}^\dagger_{\mathbf{i}\sigma} \hat{c}_{\mathbf{i}\sigma}$. The first sum is taken over all nearest neighbor pairs $\langle \mathbf{i}, \mathbf{j} \rangle$ of a two-dimensional square lattice. t is the nearest-neighbor hopping parameter which sets the energy scale ($t = 1$), with the electronic bandwidth given by $W = 8t$. At each site are local harmonic oscillators of frequency ω_0, with independent degrees of freedom $\hat{X}_{\mathbf{i}} = \sqrt{\frac{1}{2\omega_0}} \left(\hat{a}^\dagger_{\mathbf{i}} + \hat{a}_{\mathbf{i}} \right)$ and $\hat{P}_{\mathbf{i}} = \sqrt{\frac{\omega_0}{2}} \left(\hat{a}^\dagger_{\mathbf{i}} - \hat{a}_{\mathbf{i}} \right)$, where $\hat{a}^\dagger_{\mathbf{i}}(\hat{a}_{\mathbf{i}})$ are phonon creation (destruction) operators at site $\mathbf{i}$. The electron density $\hat{n}_{\mathbf{i}\sigma}$ couples to the displacement $\hat{X}_{\mathbf{i}}$ through a local electron-phonon coupling λ. In this work we measure the electron-phonon coupling in terms of the dimensionless quantity $\lambda_D = \lambda^2/\omega_0^2 \, W$.

We study the Holstein model using determinant quantum Monte Carlo (DQMC) simulations [40, 41]. In DQMC, the inverse temperature is expressed as $\beta = L_t \Delta\tau$, where L_t denotes the number of intervals along the imaginary time axis with discretization $\Delta\tau$. The partition function $Z = \mathrm{Tr}\, e^{-\beta \hat{H}} = \mathrm{Tr}\, e^{-\Delta\tau \hat{H}} e^{-\Delta\tau \hat{H}} \ldots e^{-\Delta\tau \hat{H}}$ can then be evaluated by inserting complete sets of phonon position states $|\{x_{i,\tau}\}\rangle$ at each imaginary time slice. Since the Hamiltonian is quadratic in fermionic operators, these can be traced out, giving

$$Z = \int d\{x_{i,\tau}\} e^{-S_{Bose}} [\det(M(\{x_{i,\tau}\})]^2 \quad (2)$$

where

$$S_{Bose} = \Delta\tau \left[\frac{\omega_0^2}{2} \sum_{\mathbf{i},\tau} x^2_{\mathbf{i},\tau} + \sum_{\mathbf{i},\tau} \left(\frac{x_{\mathbf{i},\tau+1} - x_{\mathbf{i},\tau}}{\Delta\tau} \right)^2 \right] . \quad (3)$$

The harmonic oscillator terms in Eqn. (1) yield the 'bosonic action' term given by Eqn. (3). The partition function also includes the product of the determinant of two matrices $M_\sigma(\{x_{\mathbf{i},\tau}\})$, one for each spin species $\sigma = \{\uparrow, \downarrow\}$. These matrices depend on the phonon field $\{x_{\mathbf{i},\tau}\}$ only. However, since $\hat{X}_{\mathbf{i}}$ couples in the same manner to the two species, the matrices M_σ are identical, giving the square of a determinant. An important consequence is the absence of a sign problem at any electronic filling.

Physical quantities can be measured via Monte Carlo sampling of the phonon field $\{x_{\mathbf{i},\tau}\}$ and accumulating appropriate combinations of the fermion Green's function $\mathcal{G}_{\mathbf{ij}} = \langle c_{\mathbf{i}\sigma} c^{\dagger}_{\mathbf{j}\sigma}\rangle = [M^{-1}]_{\mathbf{ij}}$. In our work we take $\Delta\tau = 0.125$. Trotter errors arising from the discretization of the imaginary time axis are less than the statistical errors associated with the Monte Carlo sampling for the charge and pair correlations given below.

The electron-phonon coupling term gives rise to an effective attractive electron-electron interaction $U_{\text{eff}} = -\lambda^2/\omega_0^2$ which promotes the formation of local pairs. On bipartite lattices this leads to CDW order at half-filling ($\langle \hat{n}_{\mathbf{i}\uparrow} + \hat{n}_{\mathbf{i}\downarrow}\rangle = 1$) with alternating doubly occupied and empty sites favored. This occurs at $\mu = -\lambda^2/\omega_0^2$, which can be shown via a particle-hole transformation. When the system is doped away from half-filling, superconductivity can arise at sufficiently low temperature due to the electron pairs becoming increasingly mobile. In this work we study the competition between CDW and SC as electron density is varied using DQMC, for a range of inverse temperatures $\beta = T^{-1}$ as low as $\beta = 28$. We fix $\lambda_D = 0.25$ and study two fixed frequencies $\omega_0 = 1$ and $\omega_0 = 4$ for lattices sizes with linear dimension up to $L = 12$.

We characterize the nature of the charge ordering by calculating the real-space, equal time, charge density correlation function $C(\mathbf{r})$, given by

$$C(\mathbf{r}) = \langle (\hat{n}_{\mathbf{i}\uparrow} + \hat{n}_{\mathbf{i}\downarrow})(\hat{n}_{\mathbf{i}+\mathbf{r}\uparrow} + \hat{n}_{\mathbf{i}+\mathbf{r}\downarrow})\rangle, \tag{4}$$

and its Fourier transform $S(\mathbf{q})$, the CDW structure factor

$$S(\mathbf{q}) = \frac{1}{N}\sum_{\mathbf{i},\mathbf{j}} e^{i\mathbf{q}\cdot(\mathbf{i}-\mathbf{j})}\langle \hat{n}_{\mathbf{i}}\hat{n}_{\mathbf{j}}\rangle. \tag{5}$$

In the CDW ordered phase, $C(\mathbf{r})$ becomes long ranged and $S(\mathbf{q})$ grows in proportion to the lattice size $N = L^2$ at the appropriate ordering wavevector $\mathbf{q} = (q_x, q_y)$. In the absence of CDW order, the charge density correlations are short ranged and $S(\mathbf{q})$ should exhibit no lattice size dependence. The superconducting response of the system is analyzed by the s-wave pair susceptibility

$$P_s = \frac{1}{N}\int_0^{\beta} \langle \Delta(\tau)\Delta^{\dagger}(0)\rangle d\tau, \tag{6}$$

where $\Delta(\tau) = \sum_{\mathbf{i}} c_{\mathbf{i}\downarrow}(\tau)c_{\mathbf{i}\uparrow}(\tau)$. Similarly, an enhancement in the pair susceptibility and the observation of lattice size dependence in P_s as the temperature is lowered can be used to detect the onset of SC order. We use the susceptibility to study SC, as opposed to an equal time structure factor, because it provides a more robust signal which is useful for exploring off-diagonal long range order of the KT type.

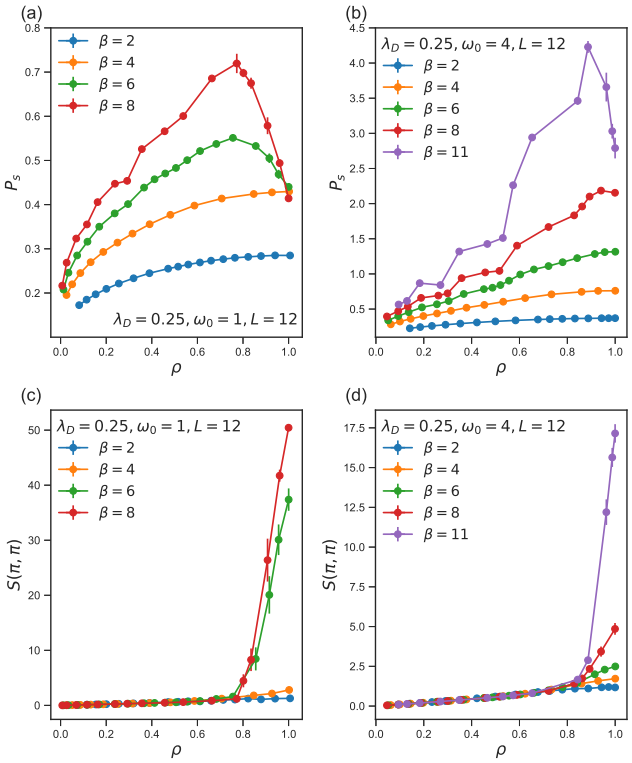

FIG. 1: (a) S-wave pair susceptibility P_s as a function of electron density ρ for $\omega_0 = 1$ and $\lambda_D = 0.25$. (b) P_s vs. ρ for $\omega_0 = 4$ and $\lambda_D = 0.25$. (c) CDW structure factor $S(\pi, \pi)$ as a function of electron density ρ for $\omega_0 = 1$ and $\lambda_D = 0.25$. (d) $S(\pi, \pi)$ vs. ρ for $\omega_0 = 4$ and $\lambda_D = 0.25$. Data are shown for a 12×12 lattice for inverse temperatures $\beta = 2$, 4, 6, 8 and 11.

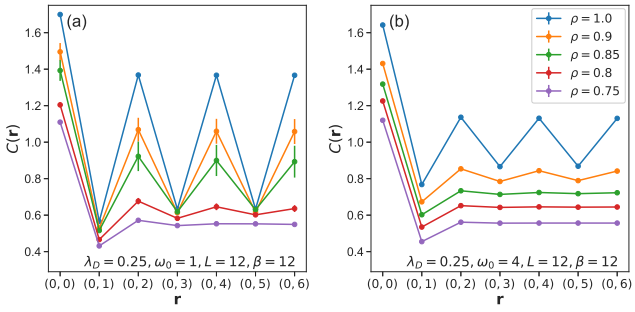

FIG. 2: (a) Charge density correlation function $C(\mathbf{r})$ as a function of site separation $\mathbf{r}$, for a 12×12 lattice at $\beta = 12$, with $\mathbf{r} = (0, 1) - (0, 6)$ in units of the lattice spacing. Results are shown for $\omega_0 = 1$ and $\lambda_D = 0.25$ for fixed electron densities: $\rho = 1$, 0.9, 0.85, 0.8 and 0.75. (b) $C(\mathbf{r})$ vs. $\mathbf{r}$ for $\omega_0 = 4$ and $\lambda_D = 0.25$.

III. RESULTS AND DISCUSSION

At half-filling, i.e. $\rho = \langle \hat{n}_{\mathbf{i}\uparrow} + \hat{n}_{\mathbf{i}\downarrow}\rangle = 1$, it is known that checkerboard CDW order dominates on the square lattice with ordering wavevector $\mathbf{q} = (\pi, \pi)$. This occurs above the inverse critical temperature $\beta_{\text{cdw}} = 6.0 \pm 0.1$ for $\omega_0 = 1$ and $\beta_{\text{cdw}} \approx 13$ for $\omega_0 = 4$, with $\lambda_D = 0.25$

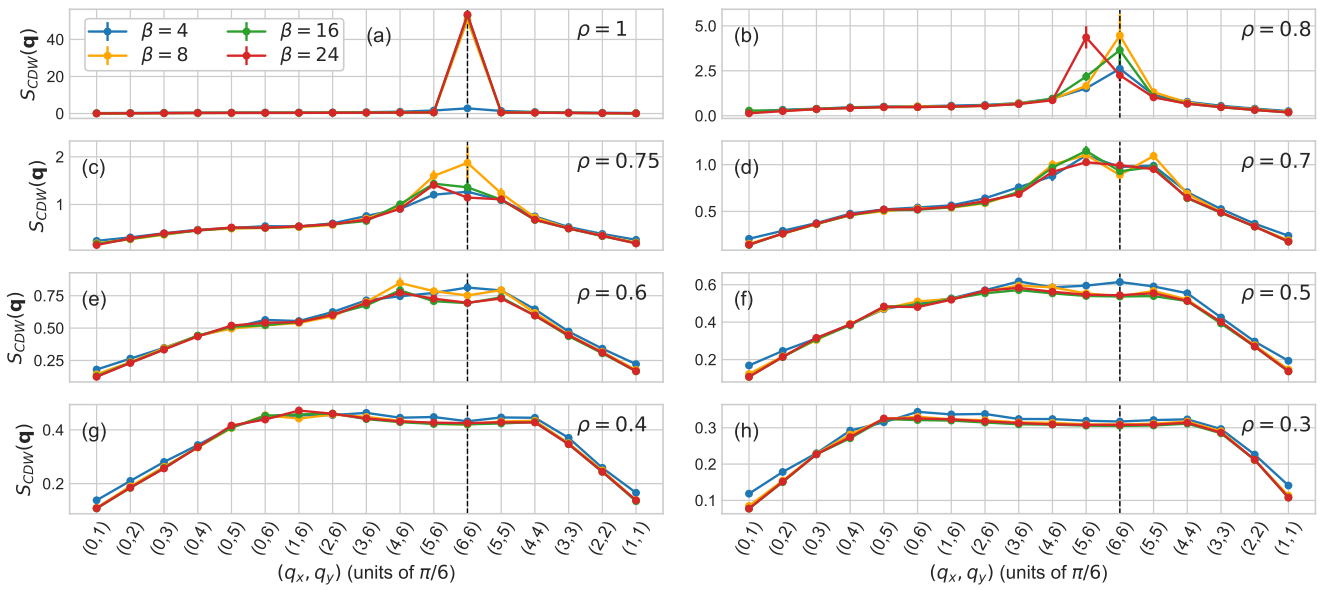

FIG. 3: Variation of $S(\mathbf{q})$ with wavevector $\mathbf{q}$ for a 12×12 lattice, for $\omega_0 = 1$, $\lambda_D = 0.25$. A triangular path through the Brillouin zone is taken from $\mathbf{q} = (0, \pi/6)$ to $(0, \pi)$ to (π, π) to $(\pi/6, \pi/6)$. Results are shown for inverse temperatures $\beta = 4, 8, 16$ and 24 for electron densities in the range $\rho = 0.3 - 1.0$, specified in the upper-right corner of plots (a)–(h). In each plot the dashed line indicates the location of $\mathbf{q} = (\pi, \pi)$.

in both cases [23]. By varying the chemical potential, we dope the system away from half-filling and study the behavior of both $S(\pi, \pi)$ and P_s as a function of electron density, as shown in Figs. 1(a)–(d) for $\omega_0 = 1$ and $\omega_0 = 4$ at $\lambda_D = 0.25$. In both cases, $S(\pi, \pi)$ is significantly enhanced at $\rho = 1$ when the inverse temperature approaches $\beta_{\rm cdw}$, but rapidly falls off when doped away from half-filling, and is highly suppressed below $\rho \approx 0.75$ for $\omega_0 = 1$. Simultaneously, the s-wave pair susceptibility becomes enhanced away from half-filling, reaching a maximum within the density range $\rho = 0.6$–0.7. When the phonon frequency is increased to $\omega_0 = 4$, P_s increases in magnitude, while $S(\pi, \pi)$ is diminished and becomes highly suppressed at a density closer to half-filling, at approximately $\rho \approx 0.85$.

The CDW ordering which occurs at half-filling above $\beta_{\rm cdw}$ on the square lattice is a checkerboard pattern of alternating doubly occupied and empty sites. This becomes evident by plotting the real-space charge density correlation function $C(\mathbf{r})$ against site separation, as shown in Fig. 2 for a 12×12 lattice at $\beta = 12$, for (a) $\omega_0 = 1$ and (b) $\omega_0 = 4$. The alternating high and low correlations at $\rho = 1$ are smoothed out as the density is lowered, with $C(\mathbf{r})$ becoming flat around $\rho \lesssim 0.75$ for $\omega_0 = 1$ and $\rho \lesssim 0.85$ for $\omega_0 = 4$. Increasing the phonon frequency inhibits CDW order, which is reflected by the smaller charge density correlations (at $\beta = 12$) for $\omega_0 = 4$, and the fact that the alternating CDW pattern is more rapidly suppressed for this frequency when doped away from half-filling.

At half-filling the square lattice exhibits perfect Fermi surface nesting (FSN) at $\mathbf{q} = (\pi, \pi)$ in the absence of any next-nearest neighbor hopping term, resulting in a peak in $S(\mathbf{q})$ at this wavevector. However when doped away from half-filling, the Fermi surface becomes distorted and perfect FSN no longer occurs. In Figs. 3(a)–(h) we show the variation of $S(\mathbf{q})$ with wavevector $\mathbf{q} = (q_x, q_y)$, taken on a triangular path through the Brillouin zone, for a 12×12 lattice at $\beta = 4$, 8, 16 and 24, for $\lambda_D = 0.25$, $\omega_0 = 1$. Results are shown for a range of electron densities from $\rho = 0.3$–1.0. $S(\mathbf{q})$ is not shown for small dopings away from half-filling. This will be further discussed in the interpretation of $\rho(\mu)$ shown in Fig. 7. Away from half-filling the peak magnitude of $S(\pi, \pi)$ is rapidly suppressed, reduced by a factor of 10 by $\rho \approx 0.8$, and falling by another order of magnitude by $\rho \approx 0.5$ (note the vertical scale of each plot).

There is an important comment to make concerning the behavior at $\rho \approx 0.8$, where the location of the peak appears to shift to the wavevector nearest to (π, π), i.e. $\mathbf{q} = (5\pi/6, \pi)$ as shown in Fig. 3(d), with the shift occurring at low temperature ($\beta \approx 24$). The magnitude of $S(5\pi/6, \pi)$ at $\rho \approx 0.8$ grows as the temperature is lowered, becoming substantially enhanced at $\beta = 24$. Although this suggests the *possible* existence of an incommensurate CDW phase at $\rho \approx 0.8$, the rather coarse discrete momentum grid $q = \frac{2\pi}{L}\{0, 1, \cdots L\}$ precludes any conclusive statement.

When the system is doped even further from half-filling, as in Figs. 3(c)–(h), we do not observe any

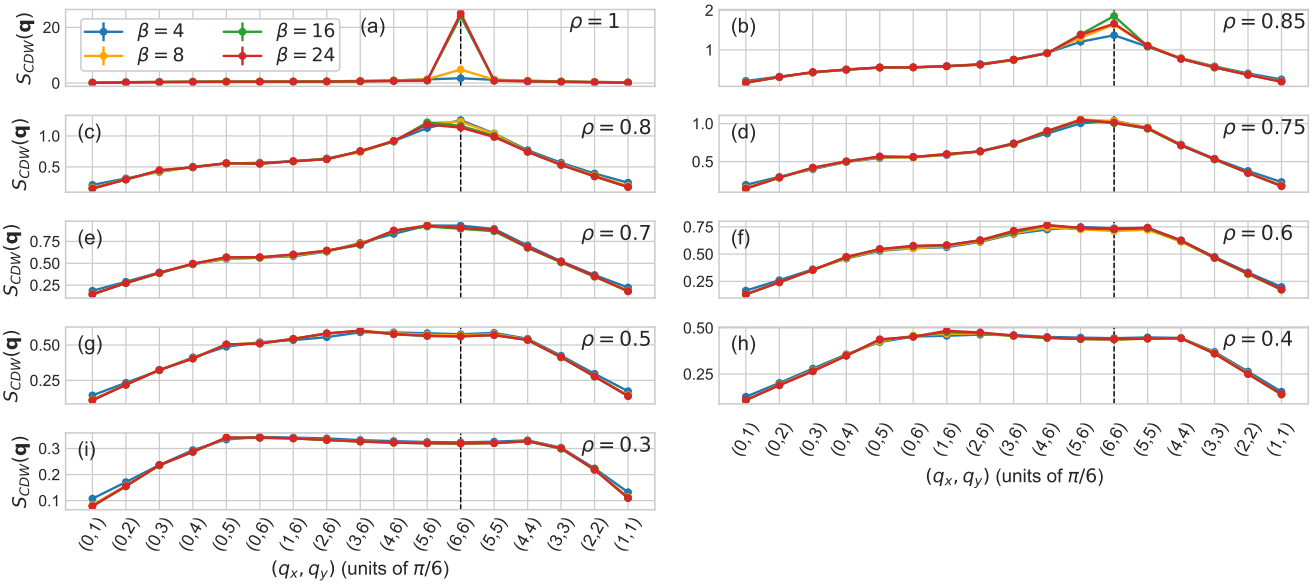

FIG. 4: Variation of $S(\mathbf{q})$ with wavevector $\mathbf{q}$ for a 12×12 lattice, for $\omega_0 = 4$, $\lambda_D = 0.25$. A triangular path through the Brillouin zone is taken from $\mathbf{q} = (0, \pi/6)$ to $(0, \pi)$ to (π, π) to $(\pi/6, \pi/6)$. Results are shown for inverse temperatures $\beta = 4, 8, 16$ and 24 for electron densities in the range $\rho = 0.3 - 1.0$, specified in the upper-right corner of plots (a)–(i). In each plot the dashed line indicates the location of $\mathbf{q} = (\pi, \pi)$.

significant enhancement in $S(\mathbf{q})$ at any wavevector as the temperature is lowered from $\beta = 4$ to $\beta = 24$. The magnitude of $S(\mathbf{q})$ remains approximately constant over this temperature range for all values of $\mathbf{q}$, as shown in Figs. 3(c)–(h) for $\rho \leq 0.75$. In particular, within the density range $\rho = 0.6$–0.7, for which we observe a peak in the s-wave pair susceptibility, we find no indication of a coexisting CDW phase for any ordering wavevector.

Increasing the phonon frequency to $\omega_0 = 4$, we find qualitatively similar results as shown in Figs. 4(a)–(i), however there is no indication of CDW ordering at any particular wavevector for any electron density, other than at $\mathbf{q} = (\pi, \pi)$ at low temperature. The magnitude of $S(\pi, \pi)$ near half filling is also considerably suppressed compared to $\omega_0 = 1$, which is expected since increasing the phonon frequency inhibits CDW order. Although the peak in $S(\mathbf{q})$ shifts to $\mathbf{q} = (5\pi/6, \pi)$ at $\rho \approx 0.8$ as the temperature is reduced, there is no significant enhancement in the magnitude of $S(\mathbf{q})$ at this wavevector as temperature is lowered from $\beta = 4$ to $\beta = 24$, in contrast to the behavior at $\omega_0 = 1$ (Fig. 3).

In order to determine the critical inverse temperature $\beta_{\rm sc}$ for the SC transition, we first tune the chemical potential to achieve a fixed target density and study P_s as a function of β, for several different lattice sizes. Since P_s appears to peak in the range $\rho = 0.6$–0.7 for $\omega_0 = 1$, $\lambda_D = 0.25$, we choose to study two fixed densities $\rho = 0.6$ and $\rho = 0.7$ for this phonon frequency. For $\omega_0 = 4$, $\lambda_D = 0.25$, since CDW correlations appear highly suppressed closer to half-filling, we fix $\rho = 0.85$ and also study $\rho = 0.6$ for comparison. In Figs. 5(a)–(d) we show $P_s(\beta)$ for lattices of linear dimension $L = 6, 8, 10$ and 12 for these four parameter sets. For each case, we find at low β (high T), P_s is relatively small and is independent of lattice size, however as the temperature is lowered, P_s grows and becomes dependent on L. This suggests the onset of the SC phase, because when correlations become long range they will be sensitive to the lattice size for a finite system. We can therefore apply a finite-size scaling analysis to confirm the existence of a critical inverse temperature $\beta_{\rm sc}$ for the SC transition, and determine its value.

In the two dimensional superconducting transition, the order parameter possesses $U(1)$ gauge symmetry and thus the universality class is the same as the 2D XY model. Hence we expect a Kosterlitz-Thouless (KT) transition to a quasi-long-range ordered phase, for which the critical exponents and scaling behavior of the order parameter are known [42]. For a finite-size system of linear dimension L, we have that

$$P_s = L^{2-\eta} f\left(\frac{L}{\xi}\right) \tag{7}$$

with $\eta = 1/4$, and as $T \to T_{\rm sc}^+$ the correlation length ξ scales as

$$\xi \sim \exp\left[A\left(T - T_{\rm sc}\right)^{-1/2}\right] \tag{8}$$

where A is a constant and $T_{\rm sc}$ is the critical temperature. Therefore near $T_{\rm sc}$, plotting $P_s L^{-7/4}$ as a function of $L \exp[-A\left(T - T_{\rm sc}\right)^{-1/2}]$ for a range of lattice sizes should

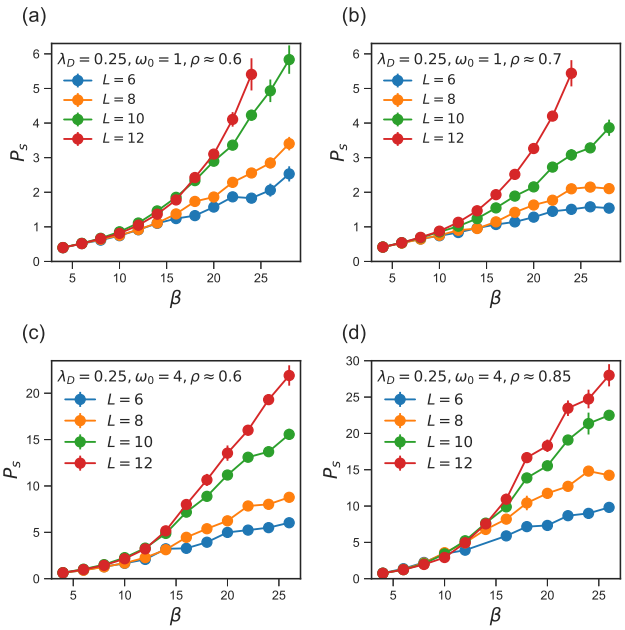

FIG. 5: S-wave pair susceptibility as a function of inverse temperature β for lattice sizes of linear dimension $L = 6$, 8, 10 and 12, for the four fixed densities studied: (a) $\rho = 0.6$ and (b) $\rho = 0.7$ for $\lambda_D = 0.25$, $\omega_0 = 1$. For increased phonon frequency $\omega_0 = 4$, we fix (c) $\rho = 0.6$ and (d) $\rho = 0.85$ with the same dimensionless coupling $\lambda_D = 0.25$ and (a,b).

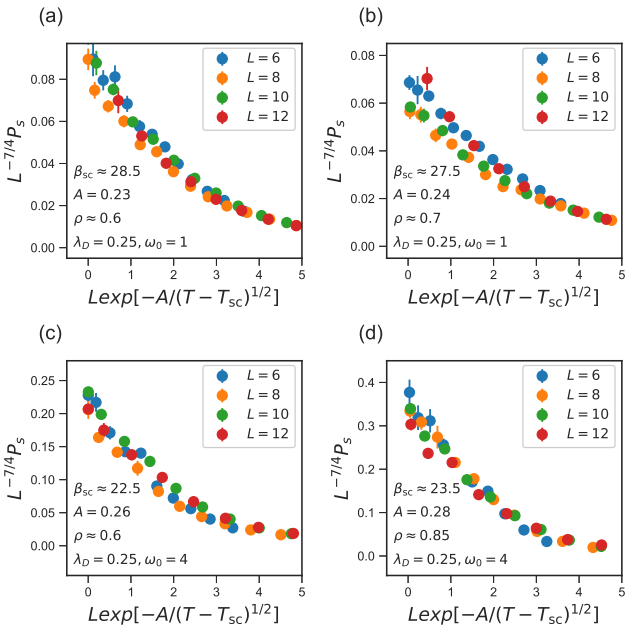

FIG. 6: Finite size scaling of the s-wave pair susceptibility data obtained for the four parameter sets shown in Figs. 5(a)–(d). The critical inverse temperature β_{sc} and scaling factor A which yields the best data collapse is indicated in the inset of each plot.

result in a data collapse onto a single universal curve, as shown in Figs. 6(a)–(d) for the four parameter sets studied. For $\lambda_D = 0.25$, $\omega_0 = 1$, we find the best data collapse occurs at $\beta_{sc} \approx 28.5 \pm 1.0$ for $\rho = 0.6$ and $\beta_{sc} \approx 27.5 \pm 1.0$ for $\rho = 0.7$. Keeping the dimensionless electron-phonon coupling fixed at $\lambda_D = 0.25$, increasing phonon frequency to $\omega_0 = 4$ raises the critical temperature, and we find the best data collapse at $\beta_{sc} \approx 22.5 \pm 1.0$ for $\rho = 0.6$ and $\beta_{sc} \approx 23.5 \pm 1.0$ for $\rho = 0.85$. Our value of β_{sc} for $\omega_0 = 1$ lies slightly below the range of $\beta_{sc} = 30$–40 suggested by Vekić et al [20], although their estimate was performed using data rather far from the scaling region. Indeed, as might be expected, to obtain a precise value we find it essential to access temperatures as close as possible to T_{sc} rather than extrapolate from higher T, as discussed in the Appendix. Meanwhile, our estimate of β_{sc} for $\omega_0 = 4$ at $\rho = 0.85$ is higher than the previous $\beta_{sc} \approx 12$ at $\rho = 0.8$. The larger values of L and β accessed in this study allow a more robust finite-size scaling for the KT transition. We also note that for the lower phonon frequency we study, for which the ME approximation would be more justifiable than for $\omega_0 = 4$, recent ME calculations [43] have estimated T_{sc} for the parameters shown in Fig. 5(a), yielding a value within approximately 10% our result.

We note that increasing phonon frequency simultaneously raises T_{sc} for the SC transition, and lowers T_{cdw} for the CDW transition at half-filling (from $T_{cdw} \approx t/6$ at $\omega_0/t = 1$ to $T_{cdw} \approx t/13$ at $\omega_0/t = 4$ [23]), illustrating the competition between SC and CDW order in the Holstein model. This is as expected since as ω_0 is lowered, the harmonic oscillators on each site become more classical, reducing quantum fluctuations. As a result, bipolarons localize more readily, enhancing CDW order [29]. Conversely, it is known that in the anti-adiabatic limit ($\omega_0 \to \infty$) the Holstein model can be mapped onto the attractive Hubbard model [18–20] with $U_{\rm eff} = -\lambda^2/\omega_0^2 = -\lambda_D W$ [44], which has been shown to possess a finite temperature superconducting KT transition away from half-filling [45–47]. Thus one expects SC correlations to be enhanced in the Holstein model at larger values of ω_0, as we have confirmed here. Furthermore, in the attractive Hubbard model, the SC and CDW correlations are degenerate at half-filling, leading to a continuous order parameter in the Heisenberg universality class and the absence of a finite-temperature transition (i.e. $T_c = 0$) in 2D. At half-filling, the CDW order parameter $S(\pi, \pi)$ is therefore reduced, with P_s increasing simultaneously in the limit $T \to 0$. We thus expect similar behavior in the Holstein model as $\omega_0 \to \infty$, which we have observed as an enhancement in P_s and a reduction in $S(\pi, \pi)$ at $\omega_0 = 4$ at half-filling, as shown in Figs. 1(a)–(d). We also note that studies of the attractive Hubbard model have found T_{sc} is maximal at around $U/t \approx -5$, for which $T_{sc}/t \approx 0.15$ occurs at a filling $\rho = 0.7$ [48]. Since this effective coupling corresponds to a larger λ_D

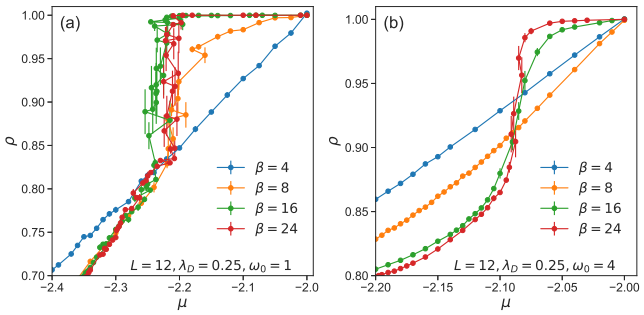

FIG. 7: Density ρ as a function of chemical potential μ approaching the CDW transition at half-filling. Results shown for $L = 12$ lattices with $\lambda_D = 0.25$, for phonon frequencies (a) $\omega_0 = 1$ and (b) $\omega_0 = 4$. The data suggest a discontinuous jump prior to entry to the incompressible CDW region. Individual data points, and their large error bars, within the discontinuous jump are shown only to emphasize the difficulty of Monte Carlo sampling in this region.

value than we study in this work, this suggests raising λ_D could enhance $T_{\rm sc}$ at large phonon frequencies. We have determined $T_{\rm sc}$ values for $-\lambda_D W = -2$ in this work, which one can compare to recent estimates of $T_{\rm sc}$ in the attractive Hubbard model [49]: for $U = -2.0$, $\beta_{\rm sc} = 19.0$ at $\rho = 0.7$, and $\beta_{\rm sc} = 13.5$ at $\rho = 0.87$, while for $U = -2.5$, $\beta_{\rm sc} = 23.0$ at $\rho = 0.5$. However, for $\omega_0 = 1$ and $\omega_0 = 4$, the actual on-site interaction will be smaller than in the anti-adiabatic limit (i.e. $|U| < 2$), giving a lower $T_{\rm sc}$, and the attractive Hubbard model thus provides an upper bound on $T_{\rm sc}$ in the Holstein model. Our estimates of $T_{\rm sc}$ at $\omega_0 = 1$ and $\omega_0 = 4$ are therefore quite consistent with those of the attractive Hubbard model.

We conclude the presentation of our results by noting that $\rho(\mu)$ appears to exhibit a discontinuous jump approaching the CDW transition at half-filling, as shown in Figs. 7(a) and (b) for $\omega_0 = 1$ and $\omega_0 = 4$. In both cases, we have that half-filling ($\rho = 1$) occurs at a chemical potential of $\mu = -\lambda^2/\omega_0^2 = -2$. Below $T_{\rm cdw}$, the formation of a plateau at $\rho = 1$ indicates the opening of the CDW gap. However, well below the transition temperature ($\beta_{\rm cdw} = 6.0 \pm 0.1$ for $\omega_0 = 1$ and $\beta_{\rm cdw} \approx 13$ for $\omega_0 = 4$) we observe a discontinuous jump in electron density as the chemical potential is varied, occurring for $\rho \gtrsim 0.8$ for $\omega_0 = 1$, and $\rho \gtrsim 0.9$ for $\omega_0 = 4$ (with $\lambda_D = 0.25$ in both cases). We note that these density ranges correspond roughly to the regions over which $S(\pi, \pi)$ grows rapidly, occurring closer to half-filling for greater ω_0, as shown previously in Figs. 1(c) and (d). The jump is less abrupt for $\omega_0 = 4$ but becomes apparent at $\beta = 24$, whereas a clear discontinuity emerges for $\beta \geq 16$ for $\omega_0 = 1$. This indicates finite temperature fluctuations smooth the jump more at higher frequencies.

In both cases, the jump is accompanied by an increase in the error in ρ for data close to half-filling, possibly indicating fluctuations of the system between densities on either side of the discontinuity. This discontinuity may be related to the zero temperature transition from SC to commensurate CDW order, which has been observed to be first order [50].

IV. SUMMARY AND CONCLUSIONS

In previous QMC studies, the CDW transition temperature $T_{\rm cdw}$ of the Holstein model at half-filling has been determined for various two-dimensional systems, including the square, honeycomb, and Lieb lattices. However, the superconducting transition away from half-filling in the square lattice has been much less well characterized, since it occurs at challengingly large values of the inverse temperature β as well as scaling in the spatial lattice size L. Moreover, away from half-filling, no analytical expression for $\rho(\mu)$ can be used to achieve a fixed target density [51], necessitating a cumbersome tuning of μ for each lattice size and β. In this work, we have studied larger systems (up to $L = 12$) and lower temperatures (up to $\beta = 28$) than in previous work, and have determined several estimates of $T_{\rm sc}$ for various electron densities (fixed via tuning the chemical potential) and phonon frequencies ω_0, through a finite-size scaling analysis of pair susceptibility. We observe the onset of SC at temperatures $T_{\rm sc} \lesssim W/160$ in each case studied. Here $W = 8\,t$ is the non-interacting bandwidth and t is the nearest neighbor hopping amplitude.

Specifically, for dimensionless electron-phonon coupling $\lambda_D = 0.25$, and phonon frequency $\omega_0/t = 1$, we estimate $T_{\rm sc} \approx W/228 = t/28.5$ for $\rho = 0.6$ and $T_{\rm sc} \approx W/220 = t/27.5$ for $\rho = 0.7$. For $\lambda_D = 0.25$, $\omega_0 = 4$, we estimate $T_{\rm sc} \approx W/180 = t/22.5$ for $\rho = 0.6$ and $T_{\rm sc} \approx W/228 = t/23.5$ for $\rho = 0.85$.

Several features illustrating the competition between CDW order and SC in the doped Holstein model emerge from our analysis. In particular, the strong checkerboard CDW order present at half-filling below $T_{\rm cdw}$ (corresponding to a peak in $S(\pi, \pi)$) is rapidly suppressed as the system is doped, with SC correlations becoming maximal in the region $\rho = 0.6$–0.7 for $\lambda_D = 0.25$, $\omega_0 = 1$. However, at an intermediate electron density of approximately $\rho \approx 0.8$, we observe evidence of a *possible* incommensurate CDW phase, with the peak in $S(\mathbf{q})$ shifting slightly from $\mathbf{q} = (\pi, \pi)$ to $\mathbf{q} = (5\pi/6, \pi)$ at low temperature. Definitive analysis of this point is precluded by the finite momentum grids currently accessible to present QMC capabilities. No evidence of a distinctly different kind of charge ordering (e.g. stripe order) is observed away from half-filling.

It is interesting to note that our estimates of $T_{\rm sc}$ in the doped Holstein model are similar in magnitude to $T_{\rm sc}$ in the half-filled case with non-zero phonon dispersion $\Delta\omega/\omega_0 = 0.1$, where DQMC simulations [23]

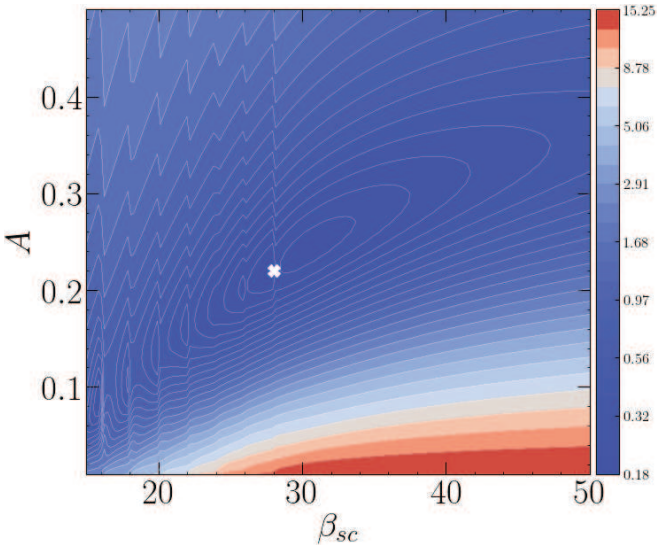

FIG. A1: Finite size scaling for $\omega_0 = 1$, $\lambda_D = 0.25$, $\rho \approx 0.6$, using data up to $\min(\beta_{sc}, 28)$. Quantity shown is the sum of squared residuals for a 4^{th} order polynomial fit to $P_s L^{-7/4}$ vs. $L \exp[A(T - T_{sc})^{-1/2}]$ using low temperature data up to $\beta = 28$. The marker indicates the best fit parameters: $A \approx 0.22$ and $\beta_{sc} \approx 28.0$.

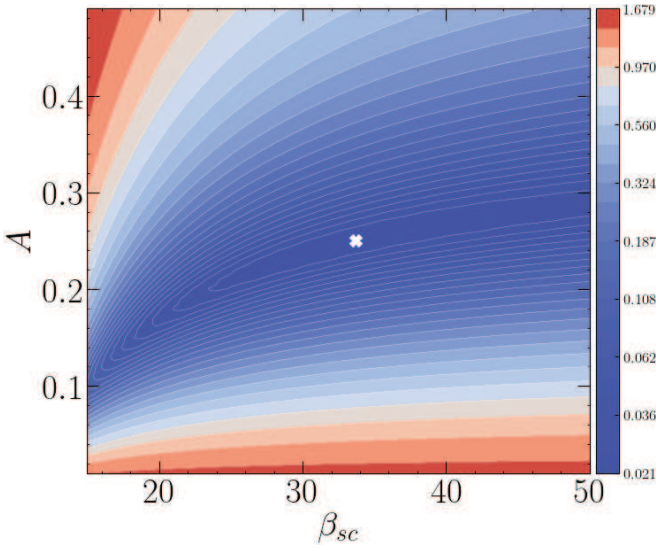

FIG. A2: Finite size scaling for $\omega_0 = 1$, $\lambda_D = 0.25$, $\rho \approx 0.6$, using data up to $\min(\beta_{sc}, 12)$, which corresponds to that available in the original studies of this model. Extrapolating T_{sc} from higher temperature, we show the sum of squared residuals for a 4^{th} order polynomial fit using data up to $\beta = 12$ only. The marker indicates the best fit parameters: $A \approx 0.25$ and $\beta_{sc} \approx 33.7$.

have determined $T_{\rm sc} \approx t/26$ for $\lambda_D = 0.25$, $\omega_0 = 4$. Further, it has been proposed [52] that an upper bound on $T_{\rm sc}$ exists which is $T_{\rm sc} \lesssim \bar{\omega}/10$, where $\bar{\omega} \leq \omega_0$ is a characteristic phonon frequency no larger than the bare phonon frequency, and that for an optimal value of λ_D, $T_{\rm sc}$ should roughly saturate at this value. Since our estimates of $T_{\rm sc}$ lie below this upper bound, this suggests it may be possible to increase the transition temperature by increasing λ_D. Recently, a QMC method based on Langevin updates of the phonon degrees of freedom [53, 54] has also made studies of the cubic Holstein model amenable to simulation, and it has been found that $T_{\rm cdw}$ at half-filling is increased roughly by a factor of two compared to various two-dimensional geometries [55]. We anticipate that in future studies of the 3D Holstein model one might similarly expect higher values of $T_{\rm sc}$ away from half-filling, since the model will exhibit a more robust transition to long-ranged superconducting order, in contrast with the KT transition in two dimensions observed in this work.

APPENDIX: EXTRAPOLATING T_{sc} FROM HIGHER TEMPERATURE

In this work, we have determined estimates of T_{sc} by accessing low temperatures (up to $\beta = 28$) close to the superconducting transition temperature, rather than extrapolating from higher T data as done in previous work. In [20], inverse temperatures up to $\beta = 12$ are accessed, and a broad range of $\beta_{sc} = 30$–40 is proposed (for $\omega_0 = 1$). To investigate how the determination of T_{sc} changes when one extrapolates from higher temperature, we have taken our data and excluded the lower temperature results, and performed Kosterlitz-Thouless scaling fits in order to mimic the capabilities of earlier work. Specifically, we have analyzed our data using only values $T \geq T_{\rm min} = 1/12$ (that is, $\beta \leq 12$).

We have fit a fourth order polynomial curve to the scaled data shown in Fig. 6, and determined the quality of these fits for various values of β_{sc} and A, shown in Figs. A1 and A2 above for the case $\omega_0 = 1$, $\rho = 0.6$. In each plot, the quantity shown is the sum of squared residuals for the polynomial fit, with lower values indicating a closer fit to the scaled data. In Fig. A1, we use all our low temperature data (up to $\beta = 28$), and Fig. A2 shows the results using data with $\beta \leq 12$. If one attempts the Kosterlitz-Thouless scaling using data with $\beta \leq 12$ only (Fig. A2), one can fit a curve to the data with relatively low error. However, in Fig. 5(a), we observed that P_s is completely independent of L for $\beta \lesssim 12$ (indicating the absence of quasi-long-range order since this is far from β_{sc}). Therefore plotting $P_s L^{-7/4}$ vs. $L \exp[A(T - T_{sc})^{-1/2}]$ yields a curve with an approximately exponential form with little to no overlap between the smallest and largest lattice sizes. In attempting to find T_{sc} from these data, we find the best collapse occurs at $A \approx 0.25$, $T_{sc} \approx 1/33.7$, and naively, using the $\beta \leq 12$ restricted data appears to provide a better fit. However, as shown in Fig. A2, the quality of the fit is essentially unchanged over a very large range of β_{sc} values (note the innermost contour which ranges from

$\beta_{sc} \approx 25$ to well beyond $\beta_{sc} = 50$). We thus find it is essential to use low temperature data as close as possible to the critical temperature (as shown in Fig. A1 which uses data with $\beta \leq 28$), not only to make the value of T_{sc} convincing, but to pin down the value more precisely than the broad range given in previous work [20].

Note that in Figs. A1 and A2 above, the scaling collapses are performed using data with inverse temperatures up to $\min(\beta_{sc}, 28.0)$ and $\min(\beta_{sc}, 12.0)$, respectively. This is because the Kosterlitz-Thouless scaling requires computing $(\frac{1}{\beta} - \frac{1}{\beta_{sc}})^{-1/2}$, and thus for each attempted collapse, data for temperatures lower than β_{sc} can not be used. Furthermore, the lack of smoothness to the contours in Fig. A1 comes from the fact that our $P_s(\beta)$ data (shown in Fig. 5) is relatively sparse, and so the best value of the scaling parameter A can change abruptly when additional data points are included in the collapse, which occurs as β_{sc} is increased.

ACKNOWLEDGMENTS

We would like to thank Steven Kivelson, Ilya Esterlis, Natanael Costa, and Rubem Mondaini for insightful comments on this work. The work of O.B. and R.S. was supported by the grant DE-SC0014671 funded by the U.S. Department of Energy, Office of Science.

[1] P. E. Kornilovitch, Phys. Rev. Lett. **81**, 5382 (1998).
[2] P. E. Kornilovitch, Phys. Rev. B **60**, 3237 (1999).
[3] A. S. Alexandrov, Phys. Rev. B **61**, 12315 (2000).
[4] M. Hohenadler, H. G. Evertz, and W. von der Linden, Phys. Rev. B **69**, 024301 (2004).
[5] L.-C. Ku, S. A. Trugman, and J. Bonča, Phys. Rev. B **65**, 174306 (2002).
[6] P. E. Spencer, J. H. Samson, P. E. Kornilovitch, and A. S. Alexandrov, Phys. Rev. B **71**, 184310 (2005).
[7] A. Macridin, G. A. Sawatzky, and M. Jarrell, Phys. Rev. B **69**, 245111 (2004).
[8] A. H. Romero, D. W. Brown, and K. Lindenberg, Phys. Rev. B **60**, 14080 (1999).
[9] J. Bonča, S. A. Trugman, and I. Batistić, Phys. Rev. B **60**, 1633 (1999).
[10] M. Hohenadler and P. B. Littlewood, Phys. Rev. B **76**, 155122 (2007).
[11] J. P. Hague and P. E. Kornilovitch, Phys. Rev. B **80**, 054301 (2009).
[12] A. R. Davenport, J. P. Hague, and P. E. Kornilovitch, Phys. Rev. B **86**, 035106 (2012).
[13] S. Li and S. Johnston, Nature Quantum Materials **5**, 40 (2020).
[14] G. Grüner, Rev. Mod. Phys. **60**, 1129 (1988).
[15] L. Gor'kov and G. Grüner, *Charge Density Waves in Solids*, vol. 25 of *Modern Problems in Condensed Matter Physics* (North Holland, 1989).
[16] A. Gabovich, A. Voitenko, T. Ekino, M. Li, H. Szymczak, and M. Pekala, Adv. Cond. Matter Phys. **2010** (2010).
[17] T. Holstein, Ann. Phys. **8**, 325 (1959).
[18] R. T. Scalettar, N. E. Bickers, and D. J. Scalapino, Phys. Rev. B **40**, 197 (1989).
[19] R. M. Noack, D. J. Scalapino, and R. T. Scalettar, Phys. Rev. Lett. **66**, 778 (1991).
[20] M. Vekić, R. M. Noack, and S. R. White, Phys. Rev. B **46**, 271 (1992).
[21] N. C. Costa, W. Hu, Z. J. Bai, R. T. Scalettar, and R. R. P. Singh, Phys. Rev. B **96**, 195138 (2017).
[22] M. Weber and M. Hohenadler, Phys. Rev. B **98**, 085405 (2018).
[23] N. C. Costa, T. Blommel, W.-T. Chiu, G. Batrouni, and R. T. Scalettar, Phys. Rev. Lett. **120**, 187003 (2018).
[24] S. Sykora, A. Hbsch, and K. W. Becker, Europhys. Lett. **85**, 57003 (2009).
[25] Y.-X. Zhang, W.-T. Chiu, N. C. Costa, G. G. Batrouni, and R. T. Scalettar, Phys. Rev. Lett. **122**, 077602 (2019).
[26] C. Feng, H. Guo, and R. T. Scalettar, Phys. Rev. B **101**, 205103 (2020).
[27] Y.-X. Zhang, H.-M. Guo, and R. T. Scalettar, Phys. Rev. B **101**, 205139 (2020).
[28] B. Cohen-Stead, N. C. Costa, E. Khatami, and R. T. Scalettar, Phys. Rev. B **100**, 045125 (2019).
[29] Z.-X. Li, M. L. Cohen, and D.-H. Lee, Phys. Rev. B **100**, 245105 (2019).
[30] A. Migdal, Zh. Eksp. Teor. Fiz. **34**, 1438 (1958).
[31] G. Eliashberg, Zh. Eksp. Teor. Fiz. **38**, 966 (1960).
[32] P. Niyaz, J. E. Gubernatis, R. T. Scalettar, and C. Y. Fong, Phys. Rev. B **48**, 16011 (1993).
[33] R. M. Noack and D. J. Scalapino, Phys. Rev. B **47**, 305 (1993).
[34] F. Marsiglio, Phys. Rev. B **42**, 2416 (1990).
[35] I. Esterlis, B. Nosarzewski, E. W. Huang, B. Moritz, T. P. Devereaux, D. J. Scalapino, and S. A. Kivelson, Phys. Rev. B **97**, 140501(R) (2018).
[36] A. S. Mishchenko, N. Nagaosa, and N. Prokof'ev, arXiv:2007.09888.
[37] A. V. Chubukov, A. Abanov, I. Esterlis, and S. A. Kivelson, Annals of Physics **417**, 168190 (2020).
[38] P. M. Dee, K. Nakatsukasa, Y. Wang, and S. Johnston, Phys. Rev. B **99**, 024514 (2019).
[39] P. M. Dee, J. Coulter, K. G. Kleiner, and S. Johnston, Commun. Phys. **3**, 145 (2020).
[40] R. Blankenbecler, D. J. Scalapino, and R. L. Sugar, Phys. Rev. D **24**, 2278 (1981).
[41] R. R. dos Santos, Braz. J. Phys. **33**, 36 (2003).
[42] J. M. Kosterlitz, J. Phys. C **7**, 1046 (1974).
[43] S. A. Kivelson and I. Esterlis, private communication.
[44] E. Berger, P. Valášek, and W. von der Linden, Phys. Rev. B **52**, 4806 (1995).
[45] R. T. Scalettar, E. Y. Loh, J. E. Gubernatis, A. Moreo, S. R. White, D. J. Scalapino, R. L. Sugar, and E. Dagotto, Phys. Rev. Lett. **62**, 1407 (1989).
[46] A. Moreo and D. J. Scalapino, Phys. Rev. Lett. **66**, 946 (1991).
[47] T. Paiva, R. R. dos Santos, R. T. Scalettar, and P. J. H. Denteneer, Phys. Rev. B **69**, 184501 (2004).
[48] T. Paiva, R. Scalettar, M. Randeria, and N. Trivedi, Phys. Rev. Lett. **104**, 066406 (2010).
[49] N. C. Costa, J. P. Lima, R. R. dos Santos, and T. Paiva, private communication.
[50] I. Esterlis, S. A. Kivelson, and D. J. Scalapino, Phys. Rev. B **99**, 174516 (2019).
[51] C. Miles, private communication.

[52] I. Esterlis, S. A. Kivelson, and D. J. Scalapino, npj Quantum Mater. **3**, 59 (2018).
[53] G. G. Batrouni and R. T. Scalettar, Phys. Rev. B **99**, 035114 (2019).
[54] G. G. Batrouni and R. T. Scalettar, J. Phys.: Conf. Ser. **1290**, 012004 (2019).
[55] B. Cohen-Stead, K. Barros, Z. Y. Meng, C. Chen, R. T. Scalettar, and G. G. Batrouni, Phys. Rev. B **102**, 161108(R) (2020).